

Influence of Tool Tip Temperature on Crater Wear of Ceramic Inserts During Turning Process of Inconel-718 at Varying Hardness

S.I.A. Qadria*, G.A. Harmain^a, M.F. Wania

^aMechanical Engineering Department, National Institute of Technology, Hazratbal, Srinagar, Kashmir, India.


Keywords:

Inconel 718
Work piece hardness
Ceramic inserts
Turning
Cutting speed
Cutting temperature
Crater wear

ABSTRACT

The present study investigates the effect of Tool Tip Temperature on crater wear of cutting inserts of ceramics in the machining of Inconel 718 with varying hardness ranges from 26 HRC to 45 HRC respectively. The effect of cutting speed on the tool-tip- temperature and crater wear has also been investigated. A series of tests were conducted to measure the tool-tip temperature during the turning process, under controllable process parameters. Aluminum - oxide ceramic (620), mixed - oxide ceramic (6050) and silicon- nitride ceramic (6190) Sandvick triangular cutting inserts were used under dry conditions of machining. It was observed, that the temperature of cutting rises monotonically due to an increase in cutting speed. Further, temperature built up on the surface near to the tooltip leads to crater wear. The significant difference was observed in crater wear for (i) varied hardness of work-piece (ii) different cutting speed and (iii) several ceramic turning inserts with fixed machining time. The al-oxide insert has shown better cutting performance low crater wear, in comparison with silicon nitride, and mixed oxide turning inserts irrespective of the hardness of work piece and also cutting speed. Further, with the increase of work piece hardness from 26 HRC to 45 HRC, i.e. 58 % of increase of hardness has a strong influence on higher temperature rise 71% at the tooltip. Further, 26 HRC possess gave better crater wear resistance.

* Corresponding author:

Syed Irshad Ahmad Qadri 
E-mail: qadrisyedirshad@gmail.com

Received: 12 October 2019

Revised: 25 March 2020

Accepted: 7 May 2020

© 2020 Published by Faculty of Engineering

1. INTRODUCTION

Metal cutting is a traditional process of machining for giving the desired shape to the components. It is a valuable addition to the mechanical parts has a significant contribution from machining operations [1,2]. Nowadays, increasing of sustainability process of machining

is becoming important. Conventional approaches of machining of thermo resistant alloys involve cutting fluid (traditional) and these have raised some environmental concerns [3-4]. Therefore, machining remains a topic of interest to researchers and industrialists keeping in view economic and environmental concerns [5]. Dry machining and environmentally cleaned is one of

the most environmentally friendly machining. Absence of lubrication, often results in decrease in tool life. Further, accompanying thermal effects close to tool-tip leads to deformation of work piece and also tool wear. In difficult to machining of materials e.g. Inconel -718, even at slow cutting speeds, considerable heat is generated at the, interface of cutting tool, and also work piece which often gets manifested as significant rise of temperature particularly at tool-tip [6]. However, due to demand for productivity and to reduce use of coolants during machining, ceramic cutting tools, are emerging as suitable candidates for high temperature applications, e.g. elevated temperatures accompanying during the turning of the nickel based alloys under dry conditions [7]. Ceramic is stable at high temperatures, besides having good characteristics and high resistance to deformation is a strong candidate for metal cutting [8]. The Inconel nickel alloy 718 is difficult to machine because it is accompanied by high-temperature rise, rapid tool wear, it has relatively low thermal conductivity. Cutting parameters strongly influence which may result in undesirable effects on the work piece, including micro structural changes [9,10]. Machining of nickel alloy 718 is unique in terms of its composition and microstructure has better nickel-based super alloy -718. Due to the extraordinary properties under elevated temperature conditions, and is widely used as a material to resist harsh and aggressive environments as in aircraft engines, turbines, and nuclear power plants [11]. Nickel alloy 718 has good thermal resistance, hardness, adequate at high temperatures and low thermal diffusivity. Besides its superior toughness, the difficulty of machining of Inconel-718 life of tool limits due to work- hardening of the alloy and may introduce metallurgical changes in work piece due to a rise in higher temperature and high cutting forces [12]. Work piece structural and surface integrities are strictly required for the final application of parts made of nickel alloys in aero engine applications [13]. These conditions of high temperatures on tool rake face combined with high mechanical loads and tool cutting edge lead to rapid tool wear with a certain probability of chipping along the cutting edge [14]. The Tool Tip Temperature is an important parameter that influences the quality of the surface finish imparted to the work piece [15]. High cutting temperature is detrimental to the cutting tool

[16,17]. Temperature rise may affect the tolerances of the machined surface. The dimensional changes in cutting tool geometry often accompanied by elongation due to thermal effects may protrude the cutting tool towards the work piece and lead to geometrical inaccuracies significantly 0.01 – 0.02 mm. Although heat dissipation occurs through flowing chip 60 – 80 % of heat from the tool-work piece interface, however, the overall generation of heat process in the metal cutting of difficult to machine alloys is highly transient and steady-state although desirable may never be attained under dry conditions. The work piece drains heat 10 – 20 %, while cutting tool dissipates heat approximately 10 % [18]. Work piece also gets deformed. The major portion of the heat flows with the chips. The build-up of temperature during high-speed cutting results in (i) rapid tool wear i.e. reduction in tool life, the cutting edges of the tool may be plastically deformed under the influence of adverse thermal gradient conditions may lead to flaking and fracturing of cutting edges [19]. Temperature measurement of the tooltip is a challenging task and it involved techniques and procedures in the unwanted material cutting process. In situ instrumentation for the measurement of temperature is difficult, as heat is generated in close vicinity of the cutting edge, and the tool is in the relative motion during the cutting [20,21]. The assessment of cutting temperature and its control is still a big challenge in particular during the machining process of the same alloys [22].

Measurement of Tool Tip Temperature in the vicinity of the tool-work piece interface includes thermocouple method, infrared radiation pyrometer method, etc. The thermocouple method is not a direct measurement technique the tooltip but permits an estimation of an overall temperature in heat affected zone close to cutting tool [23]. Tool Tip Temperature directly leads to an increase of wear and the limits tool life and may plastically damage the cutting tools, which may result in metallurgical changes of the work-piece and tool material [24]. Therefore, assessment of Tool Tip Temperature is an important parameter to maintain the good surface finish. Under steep thermal gradient conditions, the tool-chip contact may lead to higher friction (dynamic) and plastic deformation and severe wear of cutting tool [25].

The different wear mechanisms observed are abrasion wear at low cutting speed, low feed rate, and higher work piece hardness. High temperature accompanied by high cutting speed resulting in the removal of the protective layer and suppressed the BUE formation. Adhesion of work piece material followed by plastic deformation and notching was clearly visible at low work piece hardness [26]. The steady-state wear rate decreases with an increase in cutting speed, depth of cut and work piece hardness [27].

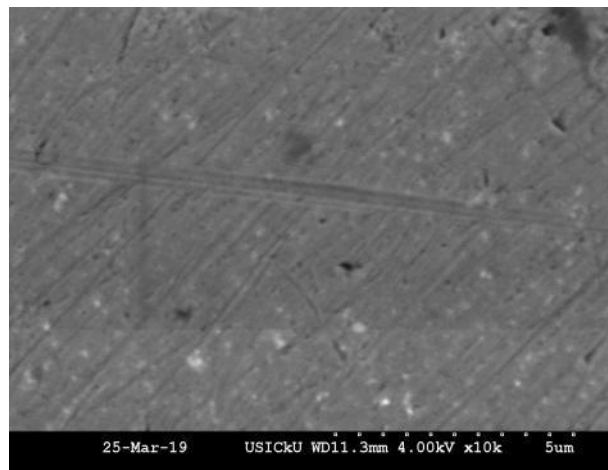
Keeping in view, the limited reported work regarding machining of Inconel alloys with regard to the Tool Tip Temperature of the cutting tool and also wear of the tools. The main aim of this work is to assess the effect of varying hardness from 26HRC, 35HRC and 45HRC of work piece material under various cutting speeds on tool tip temperature and tool life in turning of Inconel alloy -718 using commercialized ceramic tools, Al- oxide ceramic (620), mixed -oxide ceramic (6050) and silicon- nitride ceramic (6190) respectively of Sandvick cutting inserts of triangular shape under dry conditions. The novelty of the work is exemplified with the consideration of varying hardness of Inconel alloy in machining and proper assessment of tool-work piece interface temperature.

2. MATERIAL AND EXPERIMENTAL METHOD

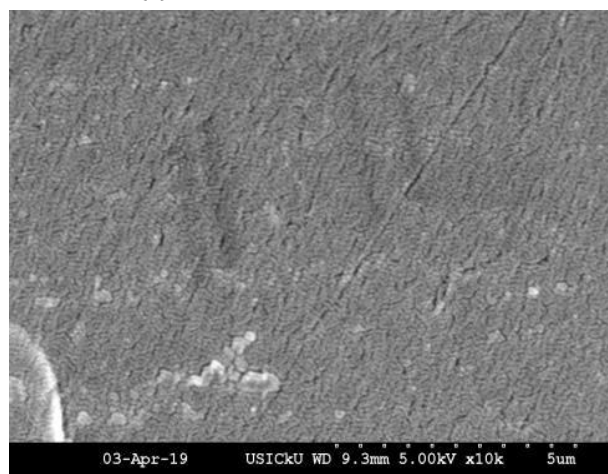
2.1 The material of the work-piece.

Several tests were conducted on rounded bars of nickel alloy -718. The varied hardness ranges from 26 HRC to 45 HRC was obtained through solution treatment. The microstructure details of work piece material are given in Figs. 1a and 1b, and Fig. 1c respectively. Figure 1(a-c) shows the effect of heat treatment on Inconel 718. These samples were solutionized at 980 °C (Fig. 1a), at 1066 °C (Fig. 1b) and at 1160 °C (Fig. 1c) for the period of 1-hour soaking and cooled by furnace cooling. The SEM surface micrograph results revealed that there is a precipitation of γ' ($\text{Ni}_3(\text{Al}, \text{Ti})$) phase which appeared as a white spot in Fig. 1(a-c) and γ'' (Ni_3Nb) intermetallic phase (Fig. 1c) appeared as a black spot in the heat-treated samples. Inconel-718 heat-treated sample at 1160 °C (Fig. 1c) has highest hardness value (HRC 45) because of the formation of two phases of γ' and γ'' precipitates, as compared the

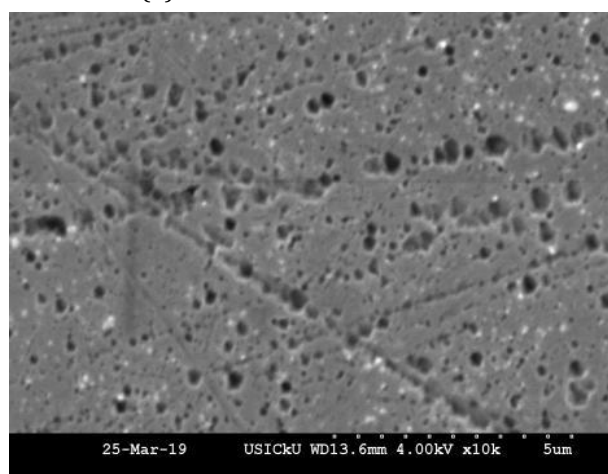
sample heat-treated at 980 °C (Fig. 1a) and 1060 °C (Fig. 1b) which has formed only one γ' phase. The EDS of Inconel 718 is shown in Fig. 2. The chemical composition of Inconel 718 was obtained and is given in Table 1.



(a) The microstructure of HRC 26



(b) The microstructure of HRC 35



(c) The microstructure of HRC 45

Fig. 1. Illustration of different SEM microstructure of Inconel alloy 718 at various heat treatment process temperatures (i) 980 °C; (ii) 1060 °C; and (iii) 1160 °C.

Table 1. Composition of IN-alloy 718.

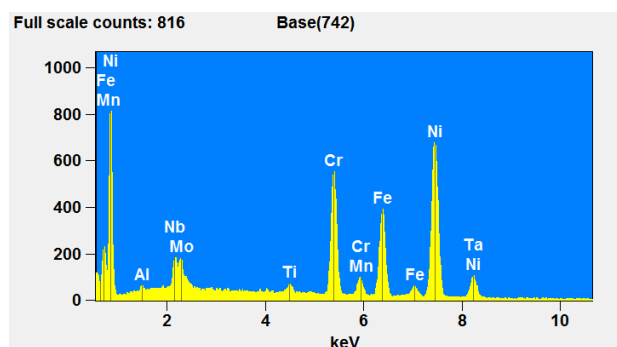
The composition is (wt%) of IN -alloy718				
Al	Ti	Cr	Mn	Fe
0.16	0.57	16.14	0.24	17.68
Ni	Nb	Mo	Ta	Total
60.69	2.49	1.57	0.46	100

2.2 Areas of applications of nickel-based alloy-718

The major area of applications of Inconel nickel-based super alloy -718 is given as under in Table 2.

Table 2. Applications of nickel alloy -718.

Applications	Components of Inconel nickel-based alloy -718
Aerospace industry	Jet engines, gas turbines, space re-entry vehicles, rocket technology reactors.
Marine Applications	Gas turbines, combustors, propeller shafts.
Power Plants (Nuclear)	Reactor Springs, fuel element recovery.
Processing Industry	Shipping Drums, Processing equipment

**Fig. 2.** EDS of Inconel nickel alloy-718.

2.3 Properties of nickel alloy -718

Inconel 718 is a nickel-based super alloy that is well suited for application requiring high strength in temperature ranges up to 1400 °F. Inconel 718 also exhibits excellent tensile and impact strength. The physical properties of Inconel 718 such as specific gravity 8.19 g/cm³ and melting range 1370 – 1430 °C. The thermal conductivity at various temp for Inconel 718 ranges 0 – 100 °C is 6.5 W/m.K.

2.4 Cutting tools

Aluminum-oxide ceramic with designation TNGA (620)160408T02520, mixed-oxide Ceramic TNGA (6050)160408S01525 and

silicon-nitride TNGA (6190)08T02520 respectively, were used for experimental machining tests of Inconel 718. Triangular type multiple lock tool-holder was used. The geometrical configuration of inserts having rake angle -10°, clearance angle 0°, the radius of the nose of insert 0.8 mm and approach plan angle 30° respectively was used for machining tests.

Table 3. Specifications of Tool-holder.

Brand Name	Dorian Tool
Cutting Angle	30°
Cutting Direction	Neutral
Item Shape	Triangle
Length	4-1/2 inches
Rake Type	Negative
Shank Height	¾ inches
Shank Type	Square
Shank Width	¾ inches
Size	½ inches

2.5 Machine details.

Tests were performed on the center lathe machine (Kirloskar make 1550) with spindle speed ranging 45 m/min to 2000 m/min) with 5HP motor drive. A sensor has been attached with the machine spindle for amassment of actual cutting speed as shown in Fig. 3a and similarly thermocouple was fixed (groove in the shim at the bottom surface of the tooltip) as shown in Fig. 3b.

2.6 Measuring devices

The instrumentation for tool and its holder consists of a thermocouple which is connected to computer collection of data pertaining to temperature in the vicinity of tool-tip during the machining operation. The spindle speed and local temperature are measured during the cutting process via a sensor and a thermocouple installed in the groove of the shim of the cutting insert as highlighted in Figs. 3a and 3b respectively.

2.7 Calibration of Thermocouple:

A calibration frame is installed on the lathe supported and positioned through a three jaw chuck, a tailstock and guide rail of the lathe. Then a spiral loading mechanism for exerting force on the simulated cutting tool in at least one of the directions i.e., X-direction, Y-direction and

the Z-direction is correspondingly installed on the frame body, and the spiral loading mechanism exerts the force on to the simulated tool according to the calibration requirement so as to calibrate the tool dynamometer. To avoid the deflection during calibration, supporting of three jaw chuck, a tail stock and guide of the lathe is required during calibration and calibration accuracy is ensured.



(a) A sensor installed for measuring the spindle speed of the machine.



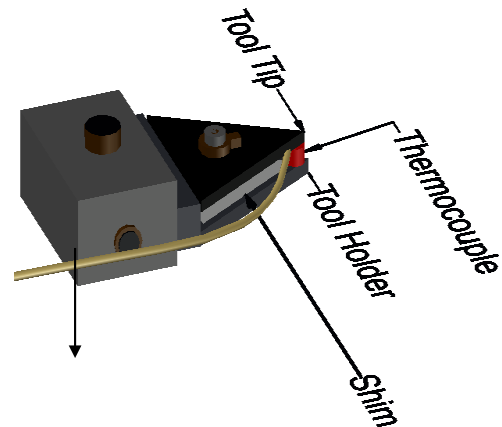
(b) Thermocouple installed in the groove on the tip of the shim of the cutting insert for measurement of tool tip temperature.

Fig. 3. Attachment of measuring devices for cutting speed and Tool -Tip- Temperature (a - b).

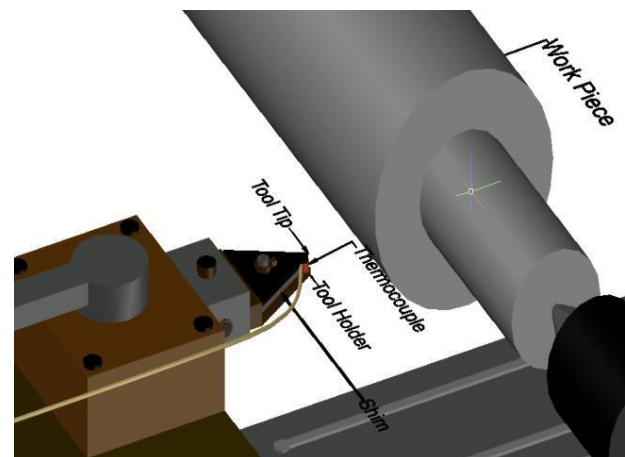


Fig. 4. Thermocouple attachment for cutting insert.

The thermocouple has a measuring range of temperatures 0 °C to 1500 °C. It is at an adequate location in the vicinity of the cutting area. The details of the insertion of the thermocouple into the shim of cutting insert are given in Fig. 4. A full assembly for the cutting operation using ceramic insert with facility for in situ measurements of in the vicinity of tool-tip is given in Fig. 5.



(a) Sectional view near thermocouple with cutting insert assembled on a tool holder.



(b) Assembly of cutting insert with thermocouple attached in a tool holder.

Fig. 5. Details of experimental set up along with tool thermocouple for tooltip temperature measurement (a - b).

To read the exact travel of cutting tool during turning, the feed sensor is installed on the machine attached with the lead screw. The duration of machining time for all the experimental tests was constantly fixed timing with 180 seconds. At the end of each test surfaces of the specimen have been examined. Observation of cutting tooltips was carried out by means of SEM equipped with an EDS system. Tool wear measurement was obtained using advanced

microscope Leica dm 6000 and equipped with the software of Leica image analysis.

Table 4. Numerical values of process parameters used in machining tests.

Process parameters (For tests)	Numerical values of process parameters
Cutting speed (v) (m / min)	145 , 230 and 360
Feed rate (f) (mm/rev)	0.19(constant)
Depth of cut(a_p) (m m)	0.3(constant)
Duration of machining (sec.)	180 (constant)

The crater wear was examined for all cutting inserts sequentially using an optical microscope and SEM. Numerical values of input process parameters i.e. (i)cutting- speed(v) (ii) feed – rate(f),(iii) depth of cut (a_p) and cutting duration) are given in Table 4.

3. RESULT AND DISCUSSION

3.1 Measurement of the tool tip temperature

The measurement of temperature in the vicinity of the tooltip for the turning process was performed under ambient conditions to determine variation in it by changing parameters cutting speed, work piece material (varied hardness) and cutting tool (different ceramic cutting inserts) respectively. The experimental results were obtained for cutting temperature versus cutting speed under the varied hardness of work piece is given in Figures 6, 7 and 8 respectively.

Figures 6, 7 and 8 respectively give details of cutting temperature for a machined tool sample under three cutting speeds (i) 145 m/min, (ii) 230 m/min, and (iii) 360 m/min respectively, which clearly indicates that temperature increases gradually at all the selected parameters to a certain values in fixed machining time of 180 seconds with varied hardness of sample material i.e., 26 HRC, 35 HRC, 45 HRC range of hardness work-piece material respectively.

All three curves for various cutting speeds indicate the same trend at the beginning of

machining using the Al-oxide tool as shown in Fig. 6a. The temperature curve for cutting speed at 145 m/min rises sharply at the beginning of machining time in 20 sec. up to 54 °C and it increases gradually with machining time of more than 50 sec. up to 60 °C temperature and further the temperature curve becomes flatter in the middle part duration of machining time from 60 sec. to 120 sec. and similarly at the final stage of machining time from 125 sec. to 180 sec. the cutting temperature starts increasing gradually to higher temperatures.

However, the trend of cutting temperature at cutting speed of 230 m/ min, and 360 m /min is different comparing with the lower cutting speed at 145 m/min. The trend of increasing cutting temperature drastically increases after completion of the machining time of 20 sec. and the temperature of 74 °C and 95 °C for 230 m/min, and 360 m/min respectively were recorded as shown in Fig. 6a. However, comparing the cutting speed 145 m/min, and 230 m/min, and 360 m/min respectively the cutting temperature for machining Inconel 718 (HRC 26) using Al oxide cutting insert is higher 12 % for 360 m/min than 145 m/min as shown in Fig. 6a.

Similarly, Figs. 6b and 6c show the cutting temperature result when mixed oxide and silicon nitride cutting tools respectively were used for machining of HRC 26. It can be noticed that temperature curve in both cases increases drastically at the beginning of machining time and after some machining time, the temperature curves tend to be reasonably stable and start increasing gradually. Further, comparing Figs. 6b and 6c, with Fig. 6 a, it is apparent that the cutting temperature for mixed oxide was approximately 20 % higher than for silicon-nitride, and 30 % for Al-oxide, cutting inserts for all the higher cutting speeds.

Similarly, the graphics of Figs. 7a, 7b, and 7c and Figs. 8a, 8b, and 8c respectively, clearly indicates, that cutting temperature increases with the increase of cutting speed for all these three ceramic tools during machining of 35 HRC and 45 HRC. However, the trend of increasing cutting temperature during turning increases with the increase of work piece hardness as shown in Fig. 8.

Further, cutting temperature of 45 HRC was higher than 35 HRC, followed by 26 HRC

respectively, by an average cutting temperature was found to be 10 % higher during machining of 45 HRC than 35 HRC and 26 HRC, using Al -oxide cutting insert. Accordingly, 22 % higher cutting temperature was found as an average when used mixed- oxide insert during machining HRC 45, compared with 35 HRC, and followed by 26 HRC.

However, the chipping of mixed oxide insert was carried out at cutting speed 360 m/min at the completion of machining time 123 seconds and temperature abruptly decreases as shown in Fig. 8b. Further, the rate of increasing the cutting temperature increased with an estimated 15 % with an increase of hardness 45 HRC indicates during using silicon nitride cutting insert. Furthermore, it is evident that the temperature of the tip of the cutting tool is a key factor that accelerates the crater wear and also effects the cutting speed and productivity in machining of Inconel alloy 718 [28].

The graphics in Figs. 6, 7 and 8 (a, b, and c) respectively indicate that the temperature of tool-tip evolves and accordingly it increases due to the increase of process parameters, cutting speed and also the hardness of the material of work-piece (varied hardness). The most effective and influential parameter for assessment of the rise of temperature is the hardness of work piece material, as compared with cutting speed [29].

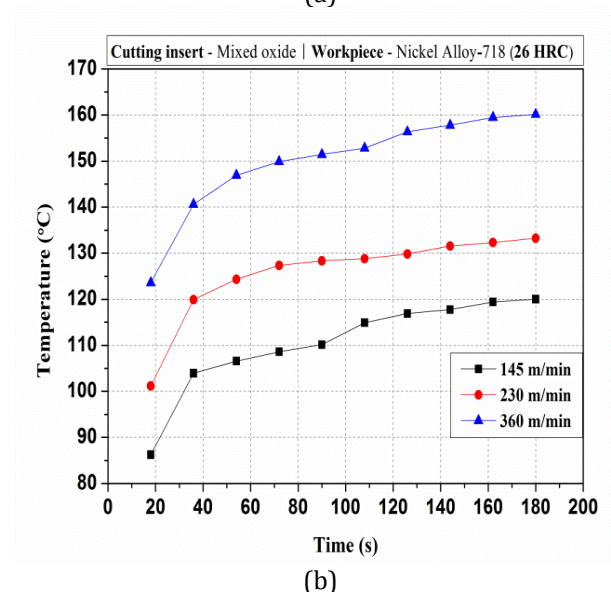
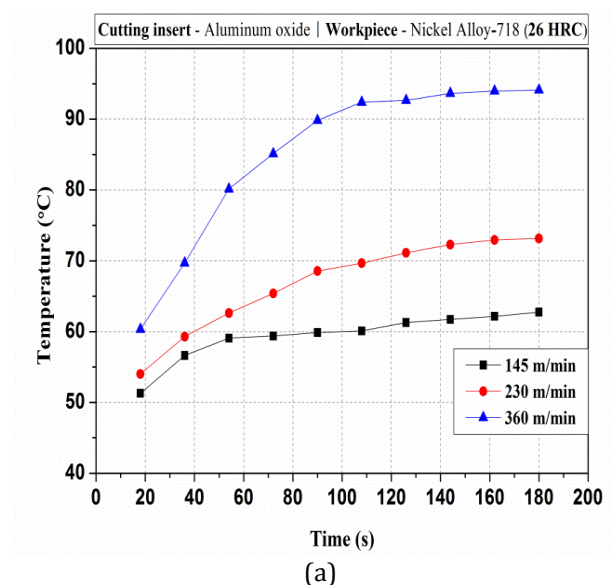
The analysis with regard to the rise of temperature of the tool and work-piece interface may be attributed to the hardness of the material i.e. Inconel 718. The build-up of temperatures is a strong function of the hardness of HRC 45. The speed of cutting has a secondary effect on the rise of temperature at the tool-tip e.g. for a 40 % increase in cutting speed an average rise in temperature was 22 % observed for all the three types of inserts. The al-oxide insert had a minimum rise in temperature followed silicon-nitride and mixed oxide inserts respectively.

The consequent effect of the rise of temperature at tool-tip is manifested in terms of wear. This wear volume for hardness HRC 45 is maximum while wear for hardness HRC 26 is minimum [30]. Besides it, high mechanical and thermal loads causing high wear tendency of ceramic cutting tools while it retains more chemically

stable and its hardness at high temperature when machining difficult to cutting materials even at lower speeds [31].

The study of generation of high temperature at localized area occurring at tool-tip is crucial because of impact of machining responses during cutting process which can be detrimental and lead to rapid wear mechanism. Reducing the temperature at the critical zone during machining may result productive and qualitative performance of the cutting tool [32].

This has significant attribution for the rise of temperature and it affects the crater wear. Therefore, it was noticed that the function of the rise of temperature during cutting of Inconel 718 is strongly correlated with the cutting speed, work piece hardness and cutting insert.



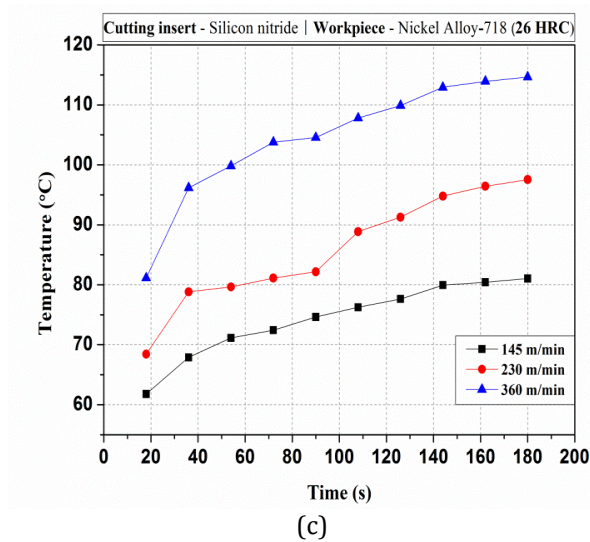


Fig. 6. Cutting temperature versus cutting speed for work- piece hardness (26 HRC) using (a) Al - oxide (b) mixed- oxide (c) silicon- nitride ceramic tools.

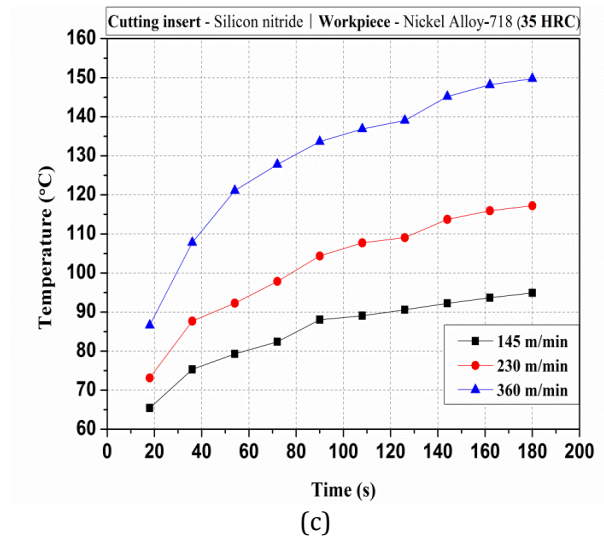
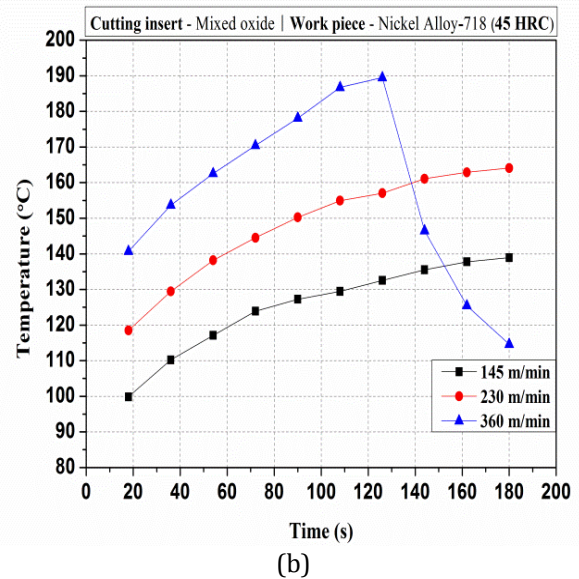
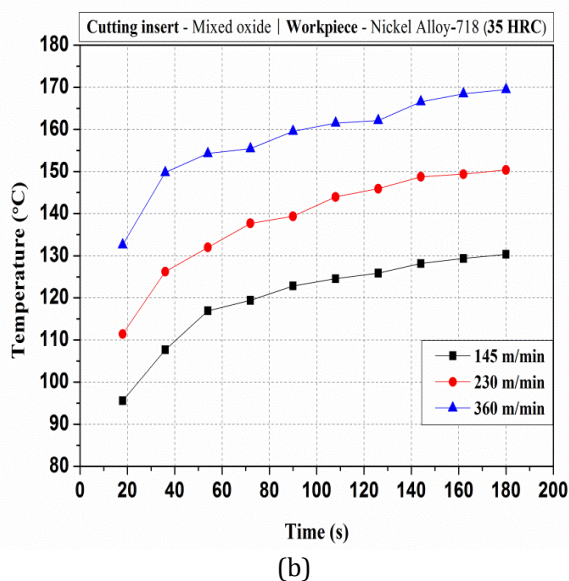
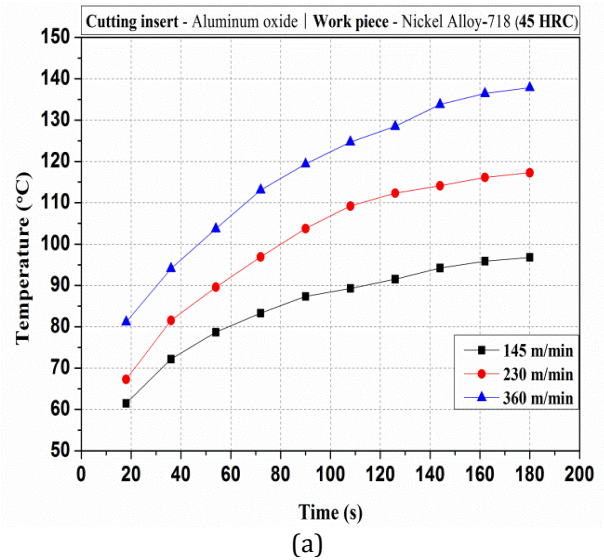
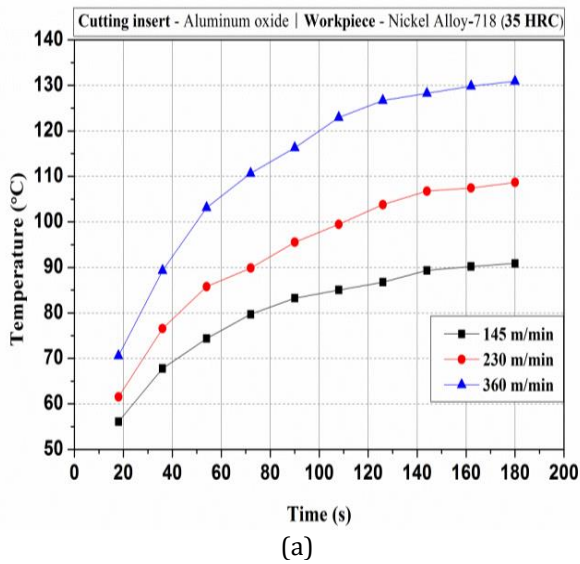


Fig. 7. Cutting temperature versus cutting - speed for work- piece hardness of (35 HRC) using (a) Al-oxide (b) mixed- oxide (c) silicon- nitride ceramic tools.



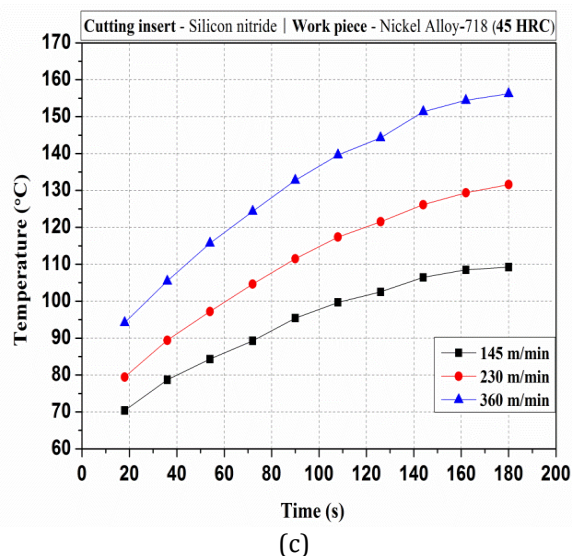


Fig. 8. Cutting temperature versus cut - speed for work- piece hardness of (45 HRC) using (a) Al-oxide (b) mixed-oxide (c) silicon -nitride ceramic tools.

The steep decrease in the temperature at the cutting speed of 360 m/min after 120 seconds is due to the sudden failure of the cutting insert during machining process.

3.2 Analysis of wear of ceramic tools

To understand the wear behaviour and tool failure modes which occur in ceramic cutting tools used in these experimental tests conducted under similar process parameter conditions. The worn-out tools were examined thoroughly on scanning-electron- microscope (SEM) and optical-microscope and has been found that adhesion, abrasion is the two wear modes which are the main cause of flank wear and failure of ceramic tools. Generally, these two wear mechanisms develop due to the high temperatures interface during cutting operations that affects the properties of the tool and work piece. Further, it is also evident the face of the rake surface of cutting tools effects by crater wear and cause of crater wear is notch and diffusion wear which results in severe crater wear and damages the rake face.

For analysis of tool wear apart from tool wear measure by tool maker's microscope (Leica DM 2500M microscope) and Scanning Electron Microscope (Hitachi) is also used. These techniques are very useful to observe the actual tool pattern and damage to the tool. SEM and microscopic images of cutting inserts were taken and evaluated to assess more effectively the determination of wear mechanisms

occurring in the ceramic inserts used in the cutting experiments and establishing wear types and consequently better evaluation of tool performance.

3.3 SEM analysis of tool wear

Figures 9, 10 and 11 respectively, show SEM images for the flank and face of the rake surfaces of all the used ceramic cutting inserts. The main focus of the present experimental study was to investigate the tool wear in particular crater wear behaviour of ceramic cutting inserts on correlation with tooltip temperature for three varied hardness Inconel 718 work piece material. Generally, during the experimental study, it has been observed that hardness and cutting speed plays an important role in the wear progression of ceramic inserts. Tool wear was characterized by the crater wear and flank wear which was observed during turning of Inconel 718 of varied hardness for cutting inserts i.e. (i) Al- Oxide, (ii) mixed- oxide and (iii) silicon- nitride respectively.

3.4 SEM Analysis of wear of the ceramic tools at speed of machining (145 m/min)

Figure 9(a-c) gives details of rake wear, and flank wear, at the speed of cutting at 145 m/min, (with constant feed and depth of cut, 0.19 mm/rev, 0.3 mm respectively). Three different cutting inserts namely Al- oxide, mixed-oxide, and silicon-oxide during machining of nickel alloy – 718 was used with varied hardness 26 HRC, 35 HRC and 45 HRC respectively. Rough flank wear is conspicuous while crater wear is in am bionic stage. Abrasive type of wear and adhesive wear on flank face surface and on rake face surface deformation and chipping off for all cutting inserts were observed. Figure 9(a-c) shows the variation of flank wear land with varied work piece hardness when machining with different cutting inserts at cutting speed 145 m/min. The flank wear did not increase quickly for all cutting tools. However, the trend can be changed when the cutting conditions work piece hardness changed. Such a situation was very obvious for the mixed oxide cutting tool as shown in Fig. 10b. The Al- oxide tool gave the best performance than other used ceramic cutting inserts. When the cutting speed was 145 m/min. The highest tool life value was achieved with Al-oxide ceramic tool at constant timing at 180 seconds.

SEM analysis of tool wear at cutting speed (145 m/min)

Work-piece material Inconel- 718 (26,35 and 45 HRC)

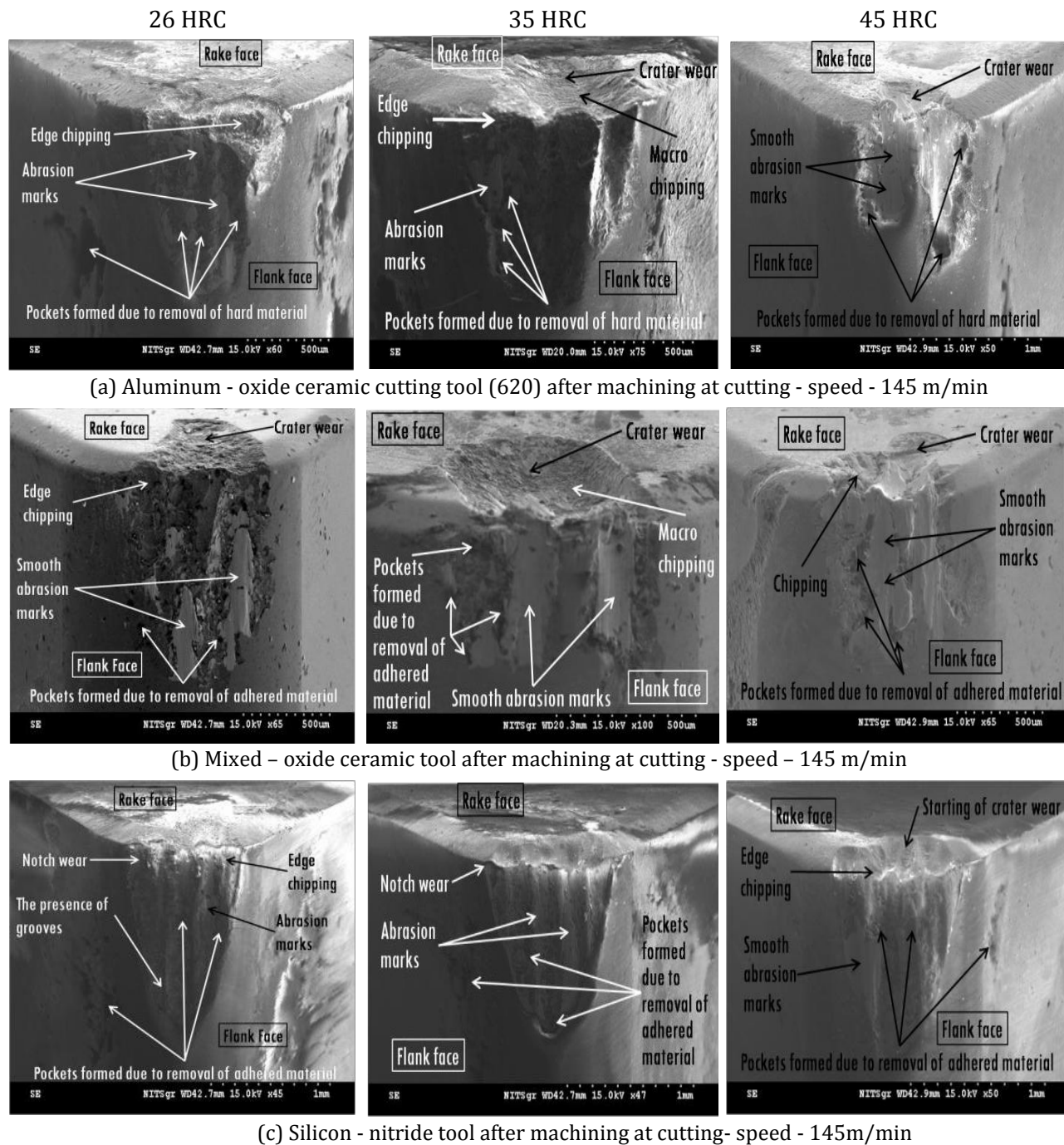
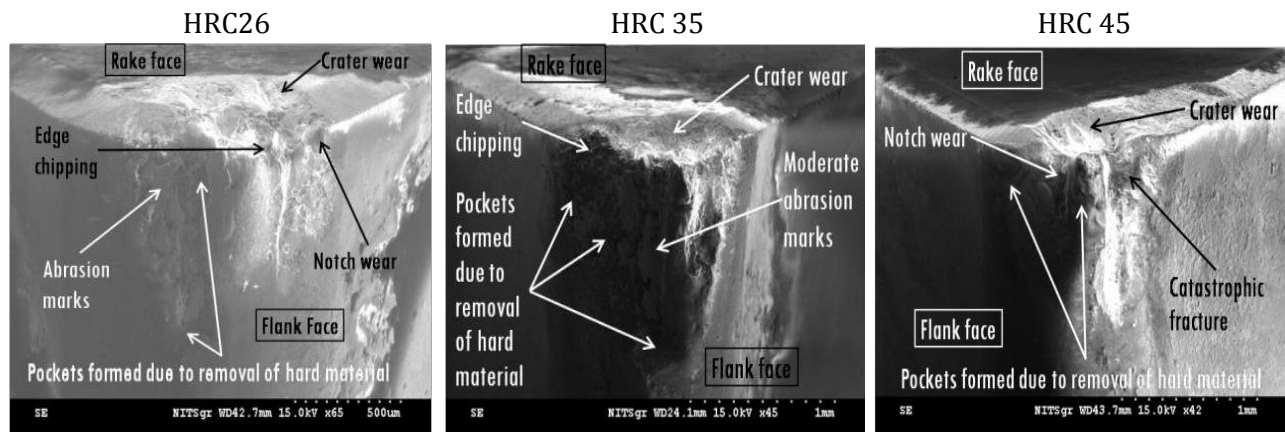


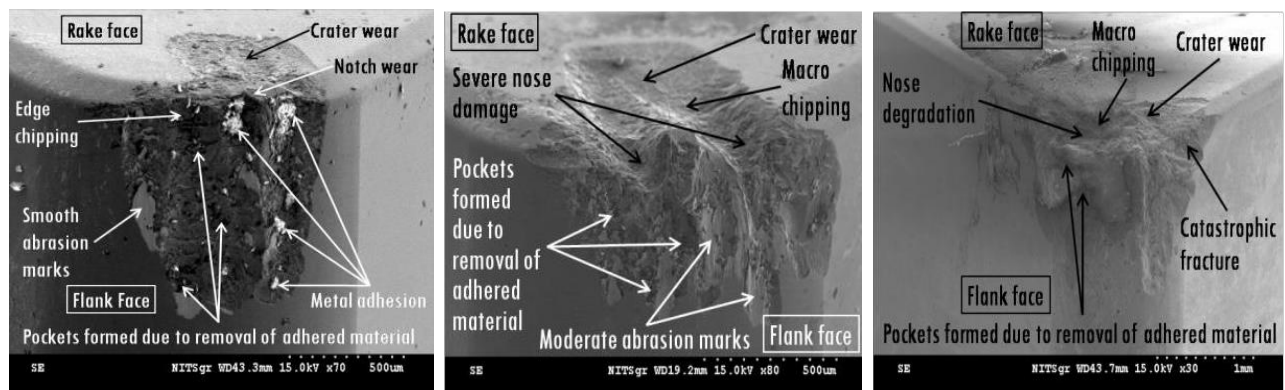
Fig. 9. SEM images of wears on (a)aluminum Oxide,(b) mixed -oxide and(c) silicon- nitride cutting inserts at cutting -speed 145m/min during turning of Inconel alloy -718 of the varied hardness of (26,35 and 45 HRC).

SEM analysis of tool wear at cutting speed (230 m/min)

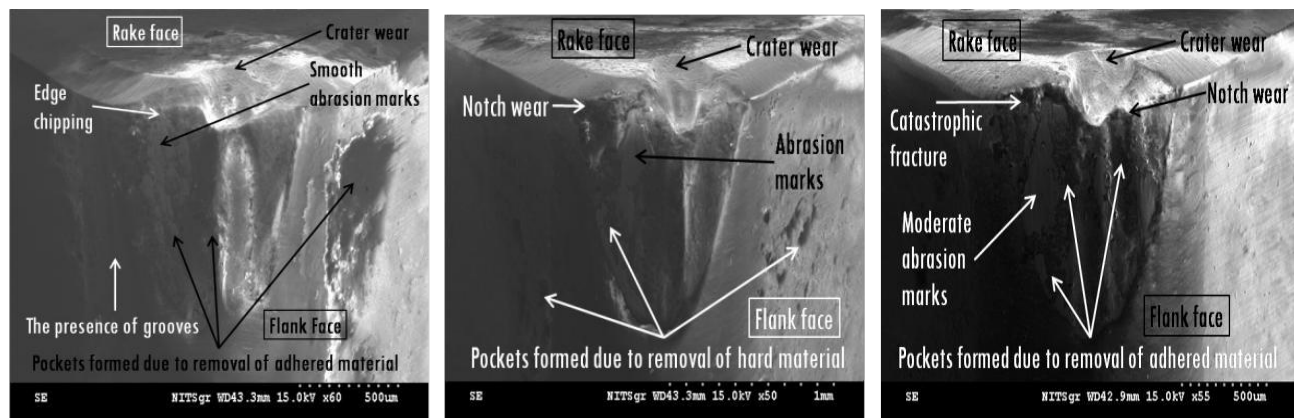
Work-piece material Inconel - 718 (26, 35 and 45 HRC)



(a) Aluminum - oxide ceramic cutting tool (620) after machining at cutting speed 230 m/min



(b) Mixed - oxide ceramic tool after machining at cutting speed 230 m/min



(c) Silicon - nitride tool after machining at cutting speed 230m/min

Fig. 10. SEM images of wears on (a) aluminum Oxide, (b) mixed - oxide, and (c) silicon - nitride cutting inserts at cutting - speed 230 m/min during turning of Inconel alloy -718 of the varied hardness of (26, 35 and 45 HRC)

SEM analysis of tool wear at cutting - speed (360 m/min)

Work-piece material Inconel -718 (26, 35 and 45 HRC)

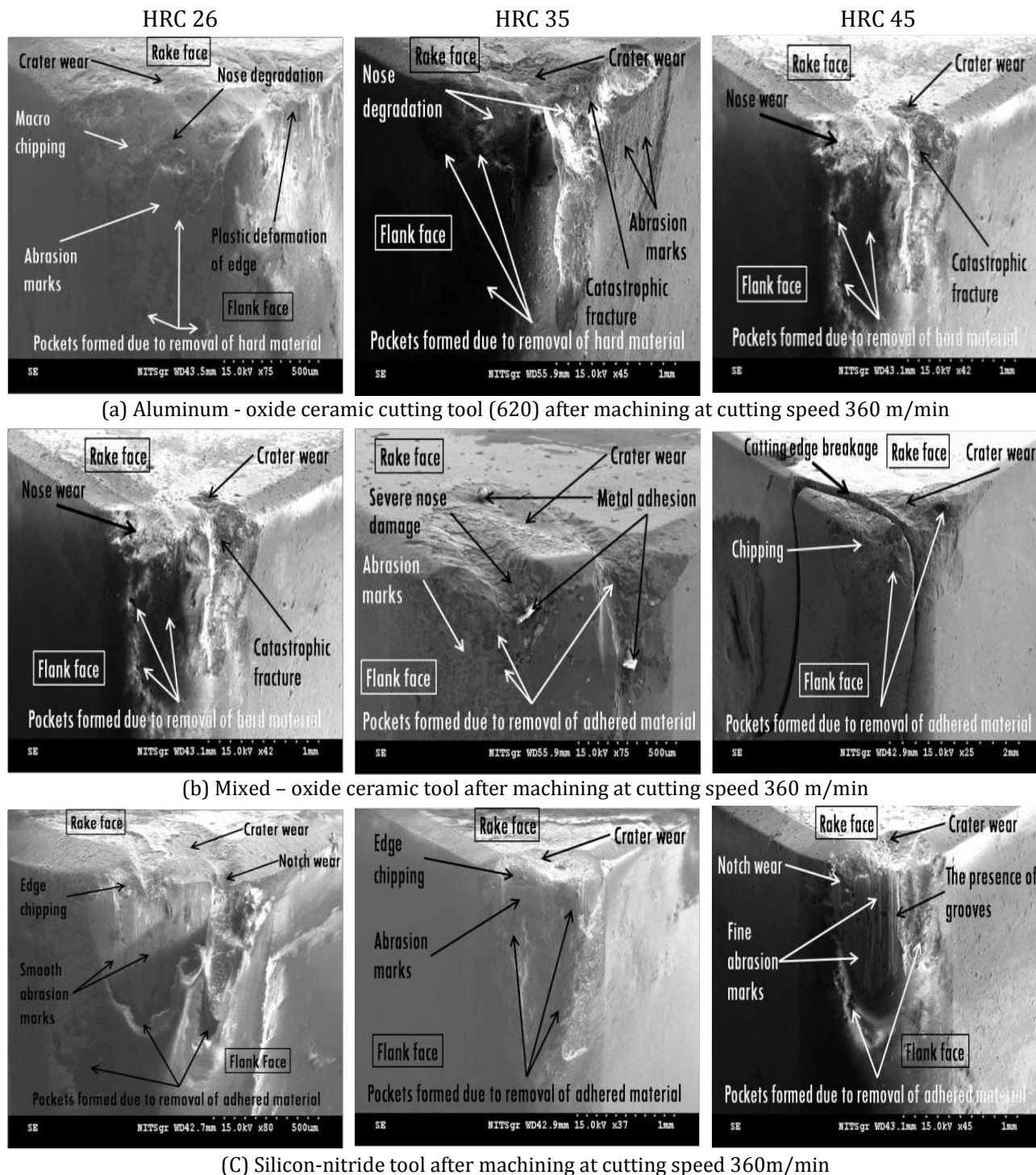


Fig. 11. SEM images of wears on (a) aluminum Oxide, (b) mixed - oxide and (c) silicon - nitride Cutting inserts at cutting - speed 360 m/min during turning of Inconel alloy -718 of the varied hardness of (26,35 and 45 HRC).

3.5 SEM analysis of tool wear at cutting- speed (360 m/min)

Figure 11 shows SEM images of wear on aluminum and mixed -oxide and silicon- nitride cutting inserts at cutting -the speed of 360 m/min

during turning of Inconel alloy - 718 of the varied hardness of 26 HRC, 35 HRC, and 45 HRC. The flank wear, for the three different hardness material conditions, is compared and it was observed that due to the increase of speed of machining the flank wear increases and as

expected work piece hardness, has an overall strong influence, on the flank and as well as on crater wear.

Figure 11(a-c) also indicates that work piece hardness has also strong effect, on notch wear while the cutting speed seems to have less effect as compared to hardness. Wider pockets, deep severe crater wear, and fracture of cutting edge at a higher cutting speed of 360 m/min during machining of (HRC 45) is conspicuous with mixed oxide as shown in Fig. 11b. Furthermore, significant wear is observed on both sides of the ceramic inserts (rake face, and flank face) and degradation leading to change of geometry of cutting inserts particularly at high material hardness and high cutting speed as shown in Figs. 9, 10 and 11 respectively (such as deep severe crater wear, notch wear, fracture of nose, and adhesive wear).

3.6 Microscopic analysis of crater wear

Tool wear during dry turning of Inconel 718 with three different ceramic tools was characterized as crater wear and flank wear which were also investigated using an optical microscope. Figures 12, 13 and 14 respectively demonstrate the optical microscopic images of rake surfaces depicting the growth of crater wear of all the three different ceramic inserts (with constant time) and for different cutting speeds. It is also evident, that increases in work piece hardness and cutting speed have a detrimental effect on crater wear of all three ceramic cutting tools.

Three different material hardness values for a particular cutting speed are given in these Figs. 12,

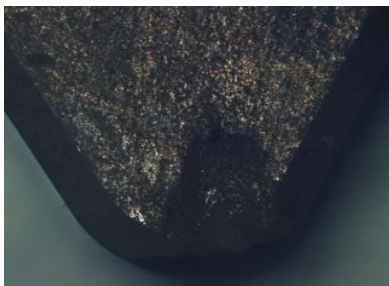
13 and 14 respectively. Crater wear of tool while machining Inconel 718 is primarily governed by the contact forces at the chip-tool contact interface region. Figures 12, 13 and 14 respectively demonstrate the optical microscope images of rake surfaces indicating the growth of crater wear of all the three different ceramic inserts with constant time duration and for different cutting speeds. It is evident that the increase of both workpiece hardness and cutting speed increased the average crater wear of all three ceramic cutting tools.

Crater wear develops on the rake face of the tool and influences the geometry of the tool-chip common surface. The important parameters affecting this wear are (i) the temperature on the common surface of tool-chip. (ii) the tendency for the chemical decomposition of cutting tool and work piece. Abrasion in the crater wear occurs through different mechanisms. In ceramic cutting tools, diffusion of particles in the work piece is the main mechanism. The process of creating crater wear involves chemical degradation of the materials of the chip and the ceramic tools that are evident for the common surface of the chip-tool. Because of the tendency to create a tribo chemical degradation in the materials of the work piece and the cutting tool chemical wear takes place. This process particularly becomes active at the high temperature generated by the cutting operation [30]. This experimental work shows that this type of wear becomes (more pronounced) at the high velocities and when the temperature on the common surface of the evolving chemical composition involves the substances of the work piece and the cutting tool.

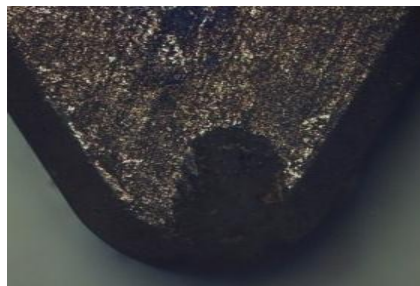
Microscopic analyses of crater wear at cutting speed (145m/min).

Work-piece material Inconel- 718 (26,35 and 45HRC)

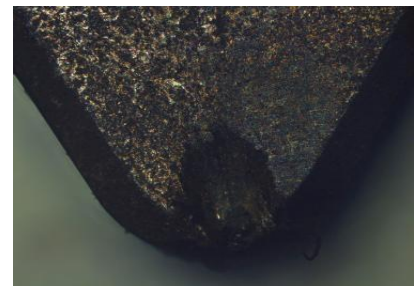
Hardness 26-HRC



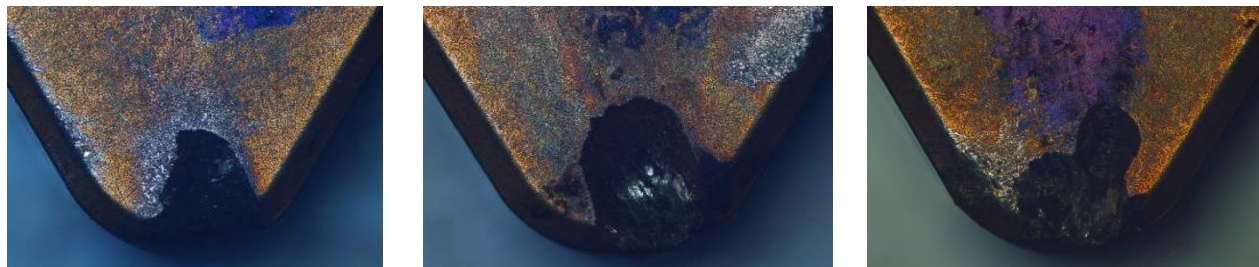
Hardness 35-HRC



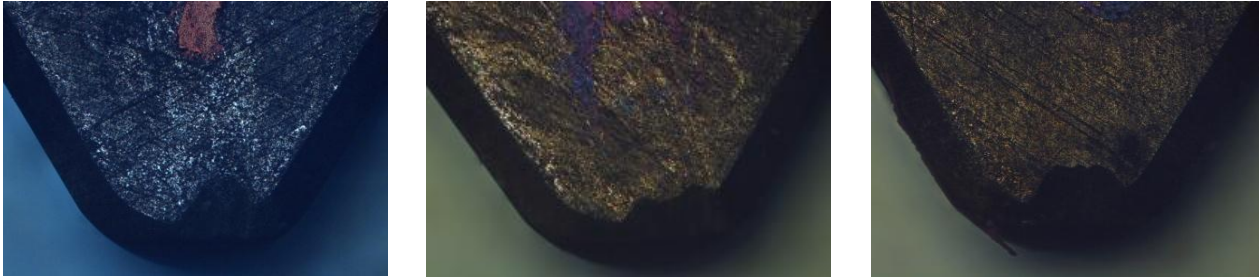
Hardness 45-HRC



(a) Aluminum - oxide tool (620) after machining(at cutting speed- 145 m/min)



(b) Mixed – oxide tool after machining (at cutting -speed 145 m/min)



(c) Silicon - nitride tool after machining at (cutting speed -145 m/min)

Fig. 12. Microscopic images of crater wear of aluminum -oxide, mixed- oxide, and silicon- nitride cutting inserts at cutting-speed -145m/min during turning of Inconel alloy -718 of the varied hardness of (26, 35 and 45 HRC).

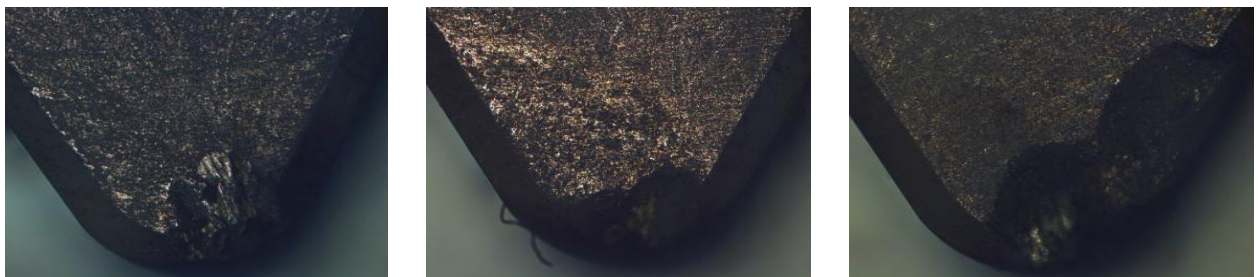
Microscopic analyses of crater wear at cutting speed (230m/min)

Workpiece material Inconel -718 (26,35 and 45HRC)

Hardness 26- HRC

Hardness 35-HRC

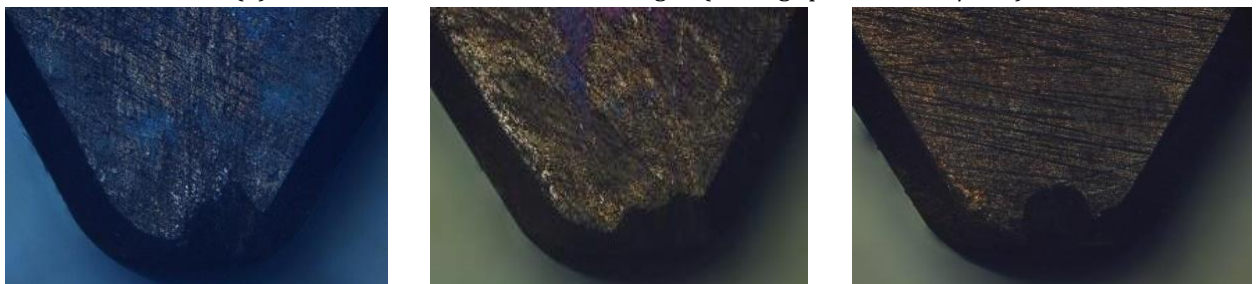
Hardness 45-HRC



(a) Aluminum-oxide tool (620) after machining at (cutting speed - 230 m/min)



(b) Mixed – oxide tool after machining at (cutting speed - 230 m/min)



(c) Silicon - nitride tool after machining at (cutting speed – 230 m/min)

Fig. 13. Microscopic images of crater wear of aluminum - Oxide, mixed, and silicon - nitride inserts at cutting-speed – 230 m/min during turning of Inconel alloy -718 of the varied hardness of (26, 35 and 45 HRC).

Microscopic analyses of crater wear at cutting speed (360m/min)

Workpiece material Inconel -718 (26, 35 and 45-HRC)

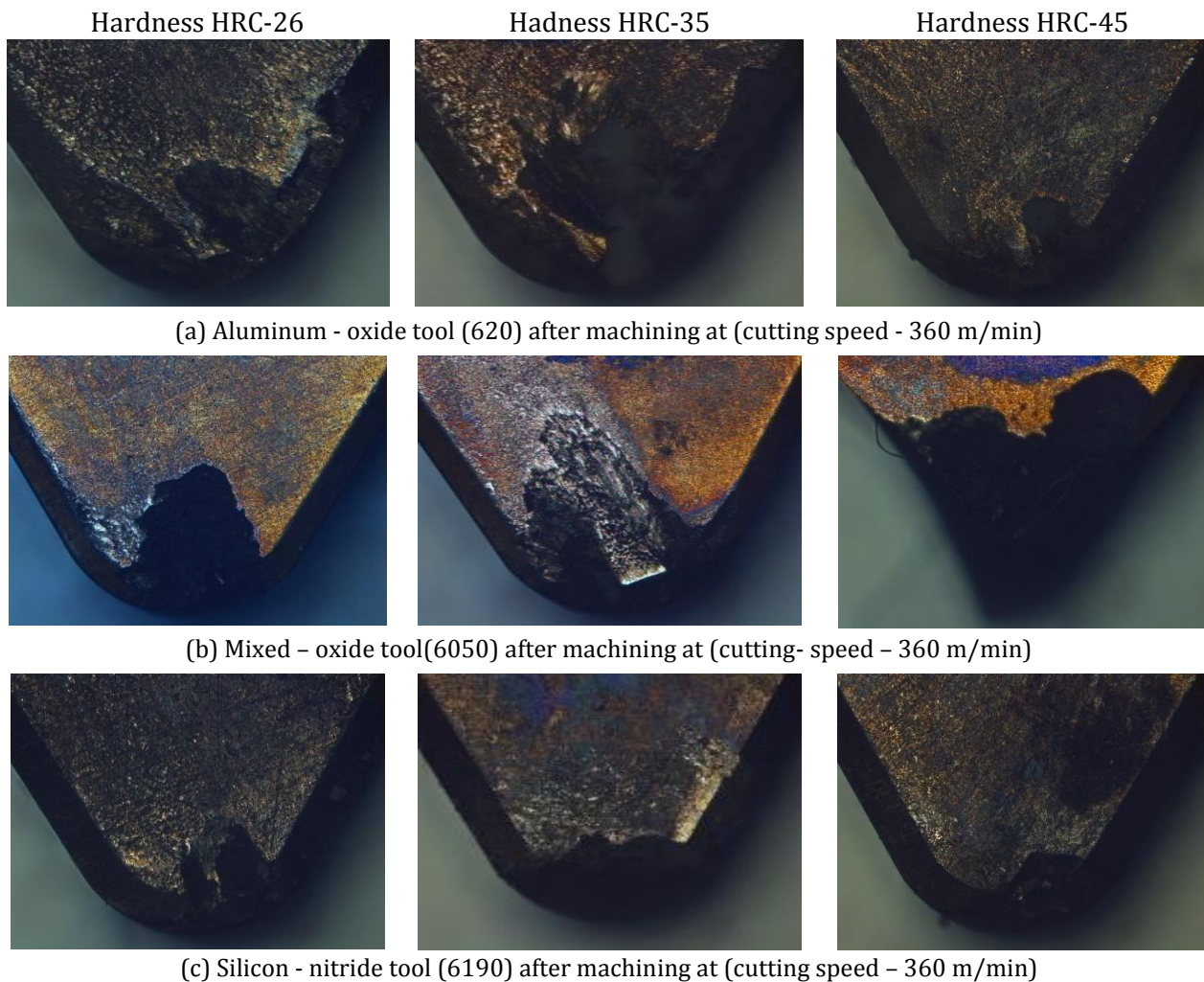


Fig. 14. Microscopic images of crater wear of aluminum - Oxide, mixed, and silicon - nitride inserts at cutting – speed – 360 m/min during turning of Inconel alloy -718 of the varied hardness of (26, 35 and 45 HRC).

4. CONCLUSION

In this experimental study, the authors studied the effects of the hardness of the material and cutting speed on ceramic turning tools with an emphasis on tooltip temperature and consequent crater wear.

- The hardness of the work piece plays a dominant role in building up of temperature at the tip of cutting tool and wear while cutting speed has a secondary role for all cuttings tools.
- Temperature near the rake face increases significantly 71 % when the material hardness increases 58 % from 26 HRC to 45 HRC coupled with increasing cutting speed, from 145 m/min to 360 m/min. The temperature at the tooltip increases with cutting speed all cutting inserts. For a 40 % increase in cutting speed an average rise in temperature was 22 % observed for all these three ceramic inserts.
- Crater wear was significantly influenced by both hardness of work piece and cutting speed despite the fact, the flank wear was mainly affected by the speed of machining and contact conditions.
- Al -oxide cutting insert displayed superior performance compared with the performance of (i) silicon- nitride and (ii) mixed- oxide cutting inserts.

- Generally, it was observed, that Crater wear increased when the hardness of work piece increased irrespective of (i) type of ceramic cutting insert and (ii) Speed of cutting used. Besides it, lower crater wear was observed for a lower value of hardness i.e., 26 HRC and followed by 35 HRC) and deep crater wear was noticed for higher range of hardness i.e., 45- HRC.
- Al-oxide ceramic cutting insert gave the best performance while the higher severe wear rate was found in mixed oxide ceramic cutting insert.

Acknowledgement

The authors wish to express gratitude and thank the Centre for research facility and Central Institute Workshop, of National Institute of Technology, Srinagar India for their support.

REFERENCES

- [1] E. Usui, T. Shirakashi, *Mechanics of machining—from descriptive to predictive theory*, On the art of cutting metals-75 years later, vol. 7, no. 1, pp. 13-55, 1982.
- [2] E. Usui, *Progress of "predictive" theories in metal cutting*, JSME international journal. Ser. 3, Vibration, control engineering, engineering for industry, vol. 31, iss. 2, pp. 363-369, 1988, doi: [10.1299/jsmec1988.31.363](https://doi.org/10.1299/jsmec1988.31.363)
- [3] R. Polvorosa, A. Suárez, L.L. De Lacalle, I. Cerrillo, A. Wretland, F. Veiga, *Tool wear on nickel alloys with different coolant pressures: Comparison of Alloy 718 and Waspaloy*, Journal of Manufacturing Processes, vol. 26, pp. 44-56, 2017, doi: [10.1016/j.jmapro.2017.01.012](https://doi.org/10.1016/j.jmapro.2017.01.012)
- [4] D. Dudzinski, A. Devillez, A. Moufki, D. Larrouquère, V. Zerrouki, J. Vigneau, *A review of developments towards dry and high speed machining of Inconel 718 alloy*, International Journal of Machine Tools and Manufacture, vol. 44, iss. 4, pp. 439-456, 2004, doi: [10.1016/S0890-6955\(03\)00159-7](https://doi.org/10.1016/S0890-6955(03)00159-7)
- [5] Y. Tamerabet, M. Brioua, M. Tamerabet, S. Khoualdi, *Experimental Investigation on Tool Wear Behavior and Cutting Temperature during Dry Machining of Carbon Steel SAE 1030 Using KC810 and KC910 Coated Inserts*, Tribology in Industry, vol. 40, no. 1, pp. 52-65, 2018, doi: [10.24874/ti.2018.40.01.04](https://doi.org/10.24874/ti.2018.40.01.04)
- [6] D. Grguraš, M. Kern, F. Pušavec, *Suitability of the full body ceramic end milling tools for high speed machining of nickel based alloy Inconel 718*, Procedia CIRP, vol. 77, pp. 630-633, 2018, doi: [10.1016/j.procir.2018.08.190](https://doi.org/10.1016/j.procir.2018.08.190)
- [7] R.M. Arunachalam, M.A. Mannan, *Performance of CBN cutting tools in facing of age hardened Inconel 718*, In Papers Presented at NAMRC, In transaction of the north American manufacturing research Institute of SME, vol. 32, pp. 525-532, 2004.
- [8] O.S. El-Sayed, *Mathematical modelling and in-process monitoring techniques for cutting tools*, PhD thesis, University of Sheffield, 1989.
- [9] A. Iturbe, E. Giraud, E. Hormaetxe, A. Garay, G. Germain, K. Ostolaza, P.J. Arrazola, *Mechanical characterization and modelling of Inconel 718 material behavior for machining process assessment*, Materials Science and Engineering: A, vol. 682, pp. 441-453, 2016, doi: [10.1016/j.msea.2016.11.054](https://doi.org/10.1016/j.msea.2016.11.054)
- [10] J. Díaz-Álvarez, J.L. Cantero, H. Miguélez, X. Soldani, *Numerical analysis of thermomechanical phenomena influencing tool wear in finishing turning of Inconel 718*, International Journal of Mechanical Sciences, vol. 82, pp. 161-169, 2014, doi: [10.1016/j.ijmecsci.2014.03.010](https://doi.org/10.1016/j.ijmecsci.2014.03.010)
- [11] R.G. Carlson, *Machining Characteristics of Alloy 718*, Superalloys 718, 625, 706 and Various Derivatives, edited by E.A. Loric, The minerals metals and materials society, pp. 839-844, 1994.
- [12] M. Rahman, W.K.H Seah, T.T Teo, *The Machinability of Inconel 718*, Journal of Materials Processing Technology, vol. 63, iss. 1-3, pp. 199-204, 1997, doi: [10.1016/S0924-0136\(96\)02624-6](https://doi.org/10.1016/S0924-0136(96)02624-6)
- [13] A. Fernández-Valdivielso, L.N. López de Lacalle, G. Urbikain, A. Rodriguez, *Detecting the key geometrical features and grades of carbide inserts for the turning of nickel-based alloys concerning surface integrity*, Proceedings of the Institution of Mechanical Engineers, Part C: Journal of Mechanical Engineering Science, vol. 230, iss. 20, pp. 3725-3742, 2016, doi: [10.1177/09544062156145](https://doi.org/10.1177/09544062156145)
- [14] A. Suárez, F. Veiga, L.N. De Lacalle, R. Polvorosa, S. Lutze, A. Wretland, *Effects of Ultrasonics-Assisted Face Milling on Surface Integrity and Fatigue Life of Ni-Alloy 718*, Journal of Materials Engineering and Performance, vol. 25, pp. 5076-5086, 2016, doi: [10.1007/s11665-016-2343-6](https://doi.org/10.1007/s11665-016-2343-6)
- [15] S.R. Carvalho, S.M.M. Lima e Silva, A.R. Machado, G. Guimarães, *Temperature determination at the chip-tool interface using an inverse thermal model considering the tool and tool holder*, Journal of Materials Processing Technology,

- vol. 179, iss. 1-3, pp. 97-104, 2006, doi: [10.1016/j.jmatprotec.2006.03.086](https://doi.org/10.1016/j.jmatprotec.2006.03.086)
- [16] S. Chinchani, S.K. Choudhury, *Evaluation of Chip-tool Interface Temperature: Effect of Tool Coating and Cutting Parameters during Turning Hardened AISI 4340 Steel*, Procedia Materials Science, vol. 6, pp. 996-1005, 2014, doi: [10.1016/j.mspro.2014.07.170](https://doi.org/10.1016/j.mspro.2014.07.170)
- [17] S. Hernandez, J. Hardell, H. Winkelmann, M.R. Ripoll, B. Prakash, *Influence of temperature on abrasive wear of boron steel and hot forming tool steels*, Wear, vol. 338-339, pp. 27-35, 2015, doi: [10.1016/j.wear.2015.05.010](https://doi.org/10.1016/j.wear.2015.05.010)
- [18] C.S. Akhil, M.H. Ananthavishnu, C.K. Akhil, P.M. Afeez, R. Akhilesh, R. Rahul, *Measurement of Cutting Temperature during Machining*, IOSR Journal of Mechanical and Civil Engineering (IOSR-JMCE), vol. 13, iss. 2, pp. 108-122, 2016, doi: [10.9790/1684-130201108122](https://doi.org/10.9790/1684-130201108122)
- [19] Y. Liu, J. Deng, F. Wu, R. Duan, X. Zhang, Y. Hou, *Wear resistance of carbide tools with textured flank-face in dry cutting of green alumina ceramics*, Wear, vol. 372-373, pp. 91-103, 2017, doi: [10.1016/j.wear.2016.12.001](https://doi.org/10.1016/j.wear.2016.12.001)
- [20] A.P. Kene, K. Orra, S.K. Choudhury, *Experimental Investigation of Tool Wear Behavior of Multi-Layered Coated Carbide Inserts Using Various Sensors in Hard Turning Process*, IFAC-Papers OnLine, vol. 49, iss. 12, pp. 180-184, 2016, doi: [10.1016/j.ifacol.2016.07.592](https://doi.org/10.1016/j.ifacol.2016.07.592)
- [21] S.K. Shihab, Z.A. Khan, A. Mohammad, A.N. Siddiquee, *RSM based study of cutting temperature during hard turning with multiple layer coated carbide insert*, Procedia Materials Science, vol. 6, pp. 1233-1242, 2014, doi: [10.1016/j.mspro.2014.07.197](https://doi.org/10.1016/j.mspro.2014.07.197)
- [22] A. Suárez, L.N. López de Lacalle, R. Polvorosa, F. Veiga, A. Wretland, *Effects of high-pressure cooling on the wear patterns on turning inserts used on alloy IN718*, Materials and Manufacturing Processes, vol. 32, iss. 6, pp. 678-686, 2016, doi: [10.1080/10426914.2016.1244838](https://doi.org/10.1080/10426914.2016.1244838)
- [23] R.T. Coelho, Eu-Gene Ng, M.A. Elbestawi, *Tool wear when turning hardened AISI 4340 with coated PCBN tools using finishing cutting conditions*, International Journal of Machine Tools and Manufacture, vol. 47, iss. 2, pp. 263-272, 2007, doi: [10.1016/j.ijmachtools.2006.03.020](https://doi.org/10.1016/j.ijmachtools.2006.03.020)
- [24] K.C. Ee, A.K. Balaji, I.S. Jawahir, *Progressive tool-wear mechanisms and their effects on chip-curl/chip-form in machining with grooved tools: an extended application of the equivalent toolface (ET) model*, Wear, vol. 255, iss. 7-12, pp. 1404-1413, 2003, doi: [10.1016/S0043-1648\(03\)00112-1](https://doi.org/10.1016/S0043-1648(03)00112-1)
- [25] R.T. Coelho, T. Reginaldo, Eu-Gene Ng, M.A. Elbestawi, *Tool wear when turning hardened AISI 4340 with coated PCBN tools using finishing cutting conditions*, International Journal of Machine Tools and Manufacture, vol. 47, iss. 2, pp. 263-272, 2007, doi: [10.1016/j.ijmachtools.2006.03.020](https://doi.org/10.1016/j.ijmachtools.2006.03.020)
- [26] J.S. Dureja, V.K. Gupta, V.S. Sharma, M. Dogra, *Wear mechanisms of coated mixed-ceramic tools during finish hard turning of hot tool die steel*, Proceedings of the Institution of Mechanical Engineers, Part C: Journal of Mechanical Engineering Science, vol. 224, iss. 1, pp. 183-193, 2009, doi: [10.1243/09544062JMES1691](https://doi.org/10.1243/09544062JMES1691)
- [27] J.S. Dureja, V.K. Gupta, V.S. Sharma, M. Dogra, *Wear mechanisms of TiN-coated CBN tool during finish hard turning of hot tool die steel*, Proceedings of the Institution of Mechanical Engineers, Part B: Journal of Engineering Manufacture, vol. 224, iss. 4, pp. 553-566, 2009, doi: [10.1243/09544054JEM1664](https://doi.org/10.1243/09544054JEM1664)
- [28] J.M.B. Carreiras, J.M.C. Pereira, Y.E. Shimabukuro, D. Stroppiana, *Evaluation of compositing algorithms over the Brazilian Amazon using SPOT-4 VEGETATION data*, International Journal of Remote Sensing, vol. 24, iss. 17, pp. 3427-3440, 2003, doi: [10.1080/0143116021000021251](https://doi.org/10.1080/0143116021000021251)
- [29] H.M. Lin, Y.S. Liao, C.C. Wei, *Wear behavior in turning high hardness alloy steel by CBN tool*, Wear, vol. 264, iss. 7-8, pp. 679-684, 2008, doi: [10.1016/j.wear.2007.06.006](https://doi.org/10.1016/j.wear.2007.06.006)
- [30] E. Ahmadi, R.M. Homani, S. Rahmati, *Experimental investigation and mathematical modeling of the composite ceramic cutting tools with alumina base in the machining process of PH-hardened Austenitic-ferritic (Duplex) stainless steel*, International Journal of Advanced Design and Manufacturing Technology, vol. 5, iss. 2, pp. 17-25, 2012.
- [31] A.R. Natasha, J.A. Ghani, C.H. Che Haron, J. Syarif, A.H. Musfirah, *Temperature at the Tool-Chip Interface in Cryogenic and Dry Turning of AISI 4340 Using Carbide Tool*, International Journal of Simulation Modelling, vol. 15, no. 2, pp. 201-212, 2016, doi: [10.2507/IJSIMM15\(2\)1.314](https://doi.org/10.2507/IJSIMM15(2)1.314)
- [32] D. Grguraš, M. Kern, F. Pušavec, *Cutting performance of solid ceramic and carbide end milling tools in machining of nickel based alloy Inconel 718 and stainless steel 316L*, Advances in Production Engineering & Management, vol. 14, no. 1, pp. 27-38, 2019, doi: [10.14743/apem2019.1.309](https://doi.org/10.14743/apem2019.1.309)